Prediction of Overpressure using Effective Stress and Velocity Trend Methods in Unag field Offshore Niger Delta

Unuagba, T.Peter[1], Ideozu, R.U[1], Eze, Stanley[2], Osung, E.Wilson[3], Abolarin, O. Macpaul[3]

[1]Department of Geology, University of Port Harcourt, Rivers State, Nigeria
[2]Department of Marine Geology, Nigeria Maritime University, Okerenkoko, Delta State, Nigeria
[3]Department of Petroleum Engineering and Geosciences, Petroleum Training Institute, Effurun, Nigeria

Abstract: Pore pressure act on subsurface formation fluids where hydrostatic pressures are equivalent to normal pressures, and high formation pressures are greater than normal pressure. Approach used in predicting overpressure are effective stress and velocity methods. The former employs rock stress behaviour as proxy for overpressure prediction while the later uses deviation from normal compaction trend to predict overpressure. This study demonstrates the effectiveness of integrating both methods in overpressure prediction. Well logs comprising of density, sonic and gamma ray logs from three wells Unag-001, 002 and 003 were used. Sonic logs were used to predict overpressure from velocity trend reversals, while density logs were used to generate 2D overburden trend which showed the effective stress of the wells and shale volume logs were generated from Gamma Ray logs. Shales are responsive to overpressure phenomena than sands because they are denser and characterized by low permeability, porosity and less resistive minerals, thus overpressure prediction was centred on shale deformation behaviour. Significant reduction in effective stress and shale density were used to identify overpressure zones while velocity reversal from sonic logs were used to validate this identification. Three overpressure zones A, B and C were identified across the three wells. In well-001, the top of overpressure zones A, B and C were identified at depth of 7600ft, 9200ft and 10500ft, for well-002 at 8100ft, 8700ft, 10300ft, and for well-003 at 8000ft, 10000t, 11800ft respectively. Based on our findings, loading mechanism of under compaction is deduced to be the overpressure mechanism in all the overpressure zones observed except for zone C in well-003, were overpressure is associated with unloading events.

Keywords: **Effective stress, Overpressure, Overburden trend, Normal compaction trend, Undercompaction.**

I. INTRODUCTION

Safe exploration of deep prospects of hydrocarbon will largely depend on our capability to understand the generation and distribution of overpressure inherent in sub layers of the formation of interest and how we can input this knowledge into a drilling plan, because it might be catastrophic to drill into a prospect without prior overpressure analysis of the prospect. Overpressure zones are major causes of drilling hazards and a key challenge in the exploration and exploitation programme of hydrocarbons reserves [1]. Overburden, effective stress and formation pore pressure are the three major pressures encountered within a formation. Overburden pressure or vertical stress is the weight of the overlying rock matrix and formation fluids acting on a sub layer of interest, effective stress are pressures exerted entirely onthe rock matrix, while formation pore pressure are pressures acting on formation fluids. Fluids occupy pore space between rock grain contacts and with constant deposition and burial, the pore space to grain contact ratio reduces, thereby exerting pressures on the fluids. These pressures increases linearly with depth and it is called normal pressure. The depth profile that compaction dependent geophysical logs follow under normal pore pressure conditions is called normal compaction trend (NCT) [2, 3]. However, variations in geologic activities such as undercompaction, tectonic compression, uplifts etc, may influence the magnitude of these normal formation fluid pressure [4, 5].

High formation pressures are pressures greater than normal pressure constituents at the same depth, while low formation pressure magnitudes are lower than normal pressure. Geologic activities that induce overpressure are called pressure mechanism, these mechanisms are subdivided into three categories, which includes; Loading, Unloading and Tectonic stress mechanism [7].Loading events are primary mechanism of overpressure [3], in which pore pressure builds up from disequilibrium compaction under rapid deposition and burial of sediments. The result of disequilibrium compaction is to slow down the rate of compaction, loss of porosity and increase in density and velocity, however, it does not stop the mechanical process of compaction. In this event, under compacted intervals may still follow the normal compaction pathway but the layers of interest will still exhibit larger porosity and lower velocity than a normally compacted layer at the same depth [3]. Trapped or partially expelled fluids in the pore spaces of undercompacted layers are subjected to overpressure. Unloading occurs at the top of loading events thus, they are called secondary overpressure mechanism. Unloading overpressure mechanism is identified when extreme overpressure abruptly reduces the in-situ density of the rock matrix thereby causing effective stress to reduce, invariably, this process is capable of bringing compaction process to a halt [3]. Tectonic stress mechanism occurs in

tectonic zones where the rate of fluids expulsion cannot keep up with the additional compaction created by tectonic stress [6].

Overpressured sub-layers exhibit distinct geophysical behaviours when compared tonormally pressured layers of the same depth, for example, they may have higher porosity, lower bulk density, higher poisson ration, lower effective stress and higher temperature [7].Terzaghi [8], formulated a simple compaction model which relates overburden pressure, effective stress and pore pressure in a mathematical expression. It can be expressed in words as; overburden pressure is equal to, the addition of effective stress and pore pressure. Although other advanced empirical models like Eaton [9] and Bowers [10] has been established to predict and evaluate overpressure, Terzaghi's method remains the basis for overpressure analysis. Overpressure prediction on geophysical logs is founded on the premise that compaction dependent logging tools such as density, sonic and resistivity are proxies for pore pressure [2]. The application of geophysical logs have been successfully applied in overpressure detection and prediction in the onshore portion of the Niger Delta Basin, Nigeria as seen in the works of [1, 11, 12], with a view to providing information on reducing drilling cost, improve safety and assessment of prospect risks.

In this study, effective stress and velocity trend techniques were used to delineate overpressure intervals in the study area. Effective stress are pressures exerted on the rock matrix, which are sand and shales in the case of the Niger Delta basin. Pressure cells are volume of specific sediments that approximately have the same overpressure [13]. Pressure cells in this case could be represented as sand or shale, thus the total pressure cell of a formation makes up the effective stress. Velocity method for predicting overpressure exploits deviations of formation sonic properties from an expected or normal compaction trend in the area of interest [3]. Sonic velocity is a transport geophysical property which travels at the boundary of rock layers, thus increased compaction trend leads to increase in sonic velocity with depth. Therefore, deviation of sonic velocity from its normal compaction trend at any depth of interest signifies an overpressure interval.

II. GEOLOGICAL SETTING OF STUDY AREA

The field under study 'UNAG' field is located in offshore Niger Delta Basin. The Niger Delta is the largest delta in Africa with a sub-aerial exposure of about $75,000 \text{ km}^2$ and clastic fill of about 9000 to over 12,000 m at the basin depocentre [14] and terminates at different intervals by trangressive sequence [15]. The onshore Niger Delta is situated on the Gulf of Guinea on the West coast of Africa and the portion of the province is delineated by the geology of Southern Nigeria and Southwestern Cameroon. The northern boundary is the Benin flank, an east–north-east trending hinge line south of the West African basement massif. It is also defined by outcrops of the Cretaceous on the Abakaliki high and further east–south-east by calaber flank, a hinge line bordering the adjacent Precambrian.

Three major depositional cycles have been identified within the Niger Delta; the first two involve mainly marine deposition that began with a major Paleocene marine transgression. The second of these two cycles started in late Paleocene to Eocene time, which reflects the progradation of a true delta with an arcuate wave and tide-dominated coastline. These sediments range in age from Eocene in the north to Quaternary in the south [16, 17]. Deposits of the last depositional cycle have been divided into a series of depobelts, also called depocentres or megasequences separated by major syn-sedimentary fault zones. These cycles (depobelts) are 30–60 km wide, prograde south-westward 250 km over the oceanic crust into the Gulf of Guinea and are defined by syn-sedimentary faulting that occurred in response to variable rates of subsidence and sediment supply [16]. A depobelt therefore forms the structural and depositional most active portion of the delta at each stage of its development. In the Niger Delta basin, 9000–12,000 m is the thickness range of clastic sediments that was formed due to flap of complex regression of the delta sedimentary structure [18, 19]. Identification of the Akata–Agbada system is the only single petroleum system known and it is called Tertiary Niger [19, 20].

The geology, stratigraphy and structure of the Niger Delta basin have been greatly studied by several workers [15, 21, 22, 23, 24, 25, 26]. The world energy assessment of United States (US) geological surveys ranked the Niger Delta basin as the 12th most prolific petroleum system with 2.2% of the world's oil and 1.4% of gas [19, 27]. The Niger Delta basin is made up of three formations: (1) Benin, (2) Agbada and (3) Akata Formations [15, 19]. The shallowest is the Benin Formation and it is made up of freshwater-bearing continental sands and gravels. Agbada Formation is the next on the sequence, underlying the Benin Formation; it consists of sand and shale intercalation with a thickness of about 3700 km. This forms a better representation of the actual deltic sequence and is the hydrocarbon reservoir unit of the sequence [19]. The final on the sequence is the Akata Formation with 7000 m thickness range; it is made up of shales, clays and silts. This formation is of turbidite origin [15, 19]. Overpressures in the Niger Delta have attracted the attention of operators and researchers quite early into the Oil and gas development activities in the basin where the depth of penetration of exploration wells were determined by the occurrence of first kicks in such wells. This practice seemed to be borne out of the belief that the occurrence of first kicks should mark the onset of overpressure hence the termination of drilling [28 as cited in 1].

III. MATERIALS AND METHODS

The data sets used in this study includes well log data (Density, Sonic and Gamma Ray logs) from three (3) wells identified as Unag-001, 002 and 003 wells in Unag field offshore Niger Delta.The location map of the study area is shown below (Figure 1). Data analysis was carried out using Rokdoc software application.
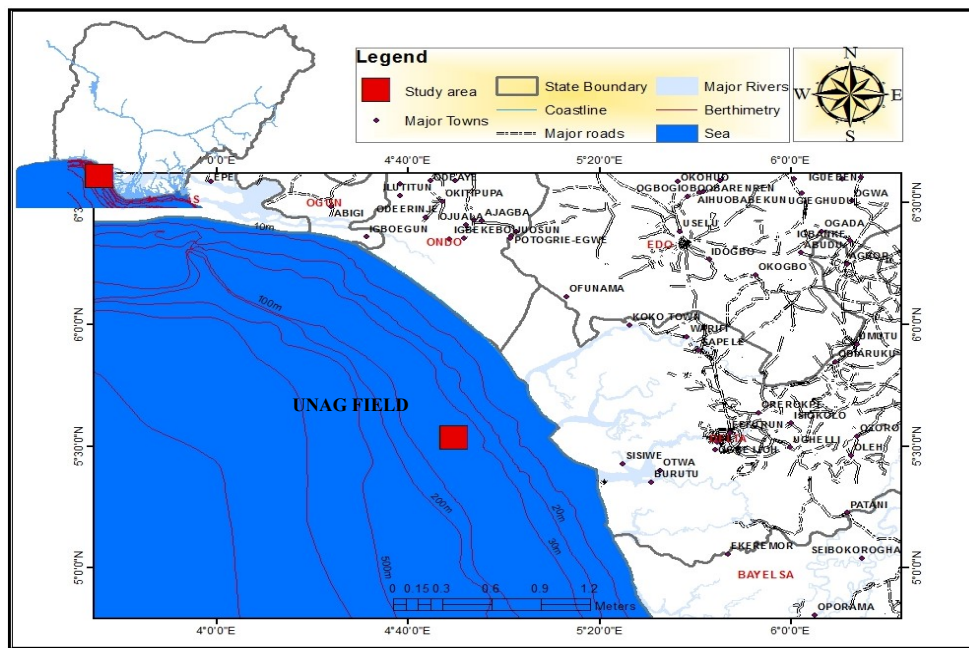
Figure 1: Location map of study area (UNAG field), offshore Niger Delta.

Overpressure prediction from well logs is based on the premise that density increases with depth in the subsurface, if this is true, then rock velocity will equally increase with depth (due to vertical stress and compaction) or follow a regular normal trend [1]. In this study, effective stress and velocity trend techniques were used to delineate the overpressure intervals within each well. Effective stress method was used to isolate possible overpressure zones, while the velocity trend method was used to pick the top of the delineated overpressure zones. Both methods were employed to supplement each other and possibly identify the mechanism of overpressure across the wells.

An exponential model (modified from Athy's [30] relationship) was used to generate the density trend within each well, which was integrated with best fit density line derived from density log data to generate the overburden trend. The empirical equation which was used to fit density as a function of depth is given as;

$$Rho(bml) = Rho_{ma} - (Rho_{ma} - Rho_{Top}) * \exp(-b * TVDBML) \qquad (1)$$

where; $Rho(bml)$ = Sediment bulk rock density as a function of depth below the mudline; Rho_{ma} = matrix density (g/cc) (2.565g/cm^3); Rho_{Top} = sediment density at mudline (g/cc); b = compaction coefficient; 0.001524 and $TVDBML$= true vertical depth below the mudline (m).

Overburden pressure gradient (ΔP_h) in psi/ft was derived from the interval overburden pressure (S) which is a variable function of depth [30]. Interval overburden pressure was calculated using the expression

$$S = 0.434 \times \rho \times \Delta h \qquad (2)$$

where; S = overburden pressure in psi, Δh = formation interval thickness (ft), ρ = density and 0.434 is the conversion factor that converts g/cc to psi.

The overburden pressure gradient (ΔP_h) in psi/ft was derived using the expression:

$$(\Delta Ph) = \frac{\Sigma S}{\Sigma h} \times 0.052 \qquad (3)$$

where; Σs = cumulative interval overburden pressure in psi, Σh = cumulative thickness in ft, and 0.052 = equivalent mud weight.

The generated overburden trend model displayed the pressure cells and density best fit line was used to demarcate sand and shale formations due to their density contrast. Significant reduction of effective stress and shale density were used to predict overpressure intervals. Shales are the major lithology for overpressure prediction because they respond more to overpressure than other rocks. Thus, pore pressure prediction centers on shale deformation behavior [2]. Shale volume logs were generated using gamma ray logs from each well to supplement results of the predicted pore pressure from 2D overburden trend, such that if density reduces or remain static in a clean shale zone, it signifies overpressure from unloading events, see Figure 2 [3].

Shale volume was derived using the expression:

$$Vshale = \frac{GR_{log} - G_{min}}{GR_{max} - GR_{min}} \qquad (4)$$
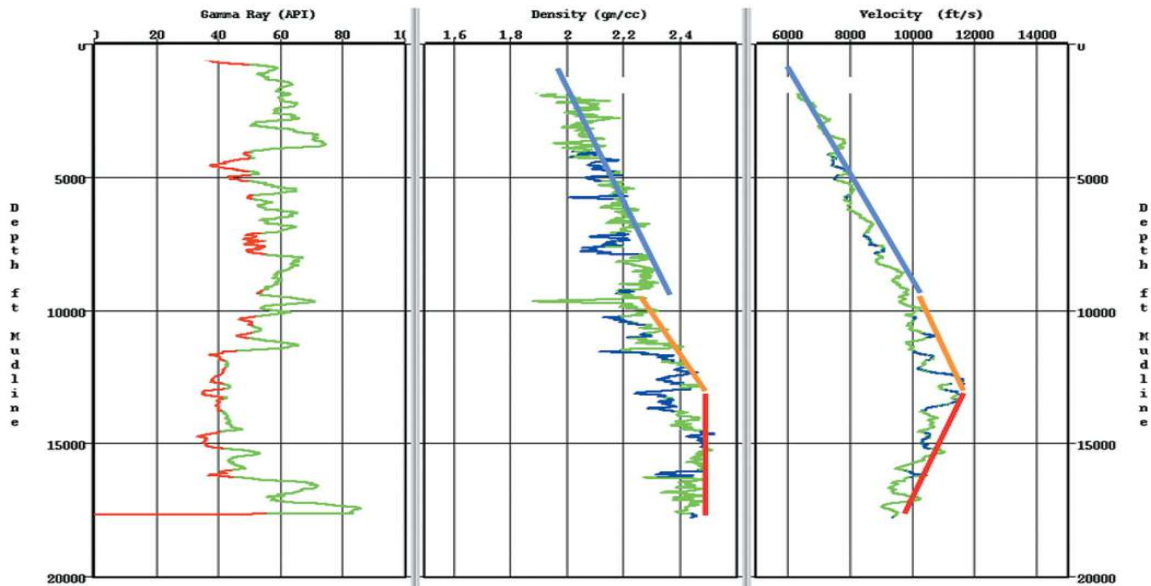
Figure 2: Density and velocity logs showing normally compacted rocks (blue line), undercompacted rocks (orange line) and unloading (red line) (After Chopra and Huffman [3]).

Velocity trend was generated using an empirical equation proposed by Zang [31], to derive normal compaction trend from sonic log, the equation is given as:

$$\Delta t_n = \Delta t_{ml} + (\Delta t_m)e^{-c} \qquad (5)$$

where; Δt_n = normal transit time reading, Δt_m = transit time in rock matrix, Δt_{ml} = mud filtrate transit time, z = depth of interest and c = compaction factor, usually derived from $\Delta t_{log}/100$, and ranges from 1.0 to 1.5.

IV. RESULTS

The results obtained in this study are shown in Figures 3-12. Overburden trend and normal compaction trend were generated from density and compressional velocity logs for wells Unag-001, 002 and 003 respectively and presented in plots. Three overpressure zones with varying thickness were identified in each well and labelled A, B and C.
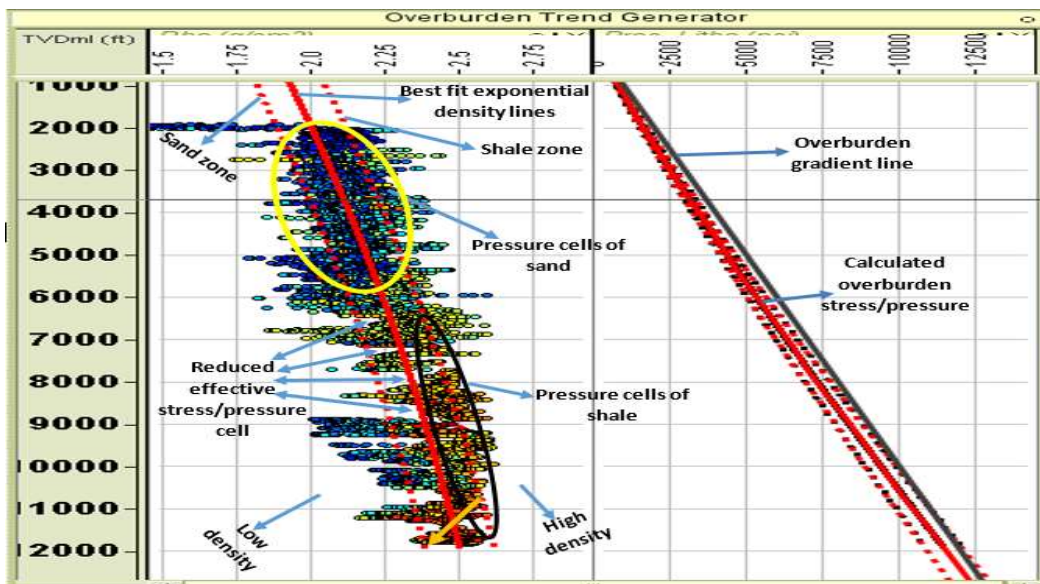
Figure 3: Overburden trend from RHOB (Density) LOG for Unag-001 well.
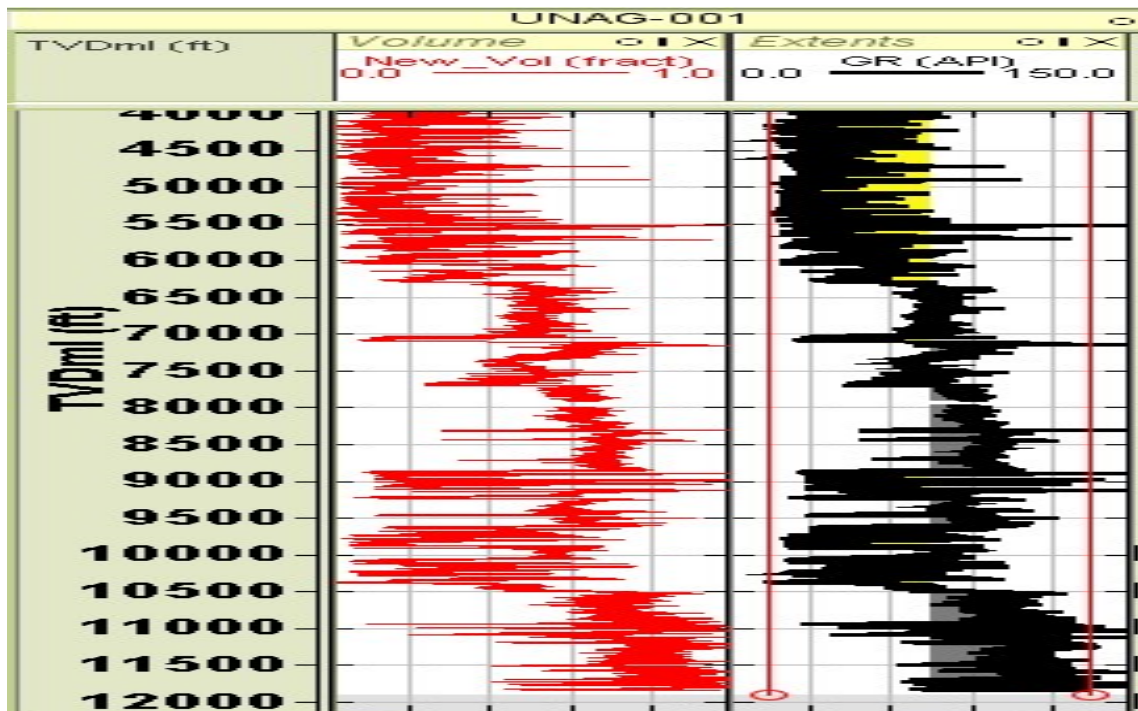
Figure 4: Shale volume log for Unag-001 well.
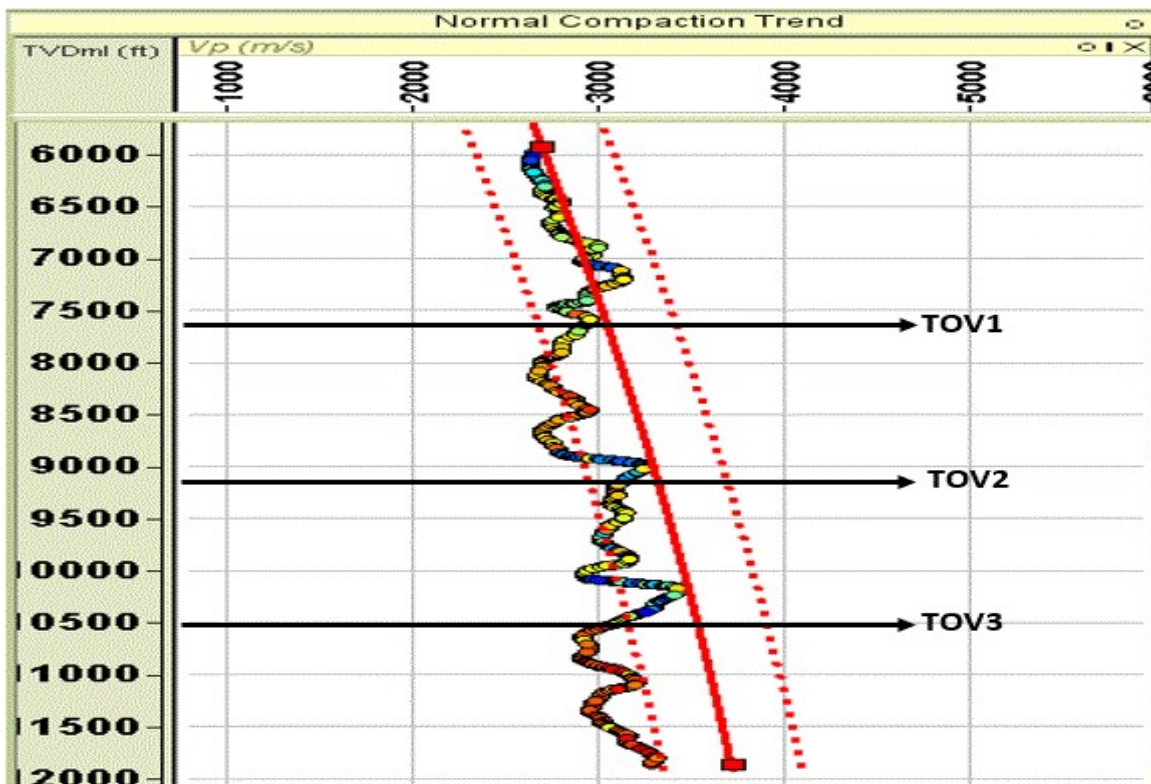
Figure 5: Normal compaction trend (NCT) from Compressional sonic velocity (Vp) log showing top of overpressure in Unag-001 Well.
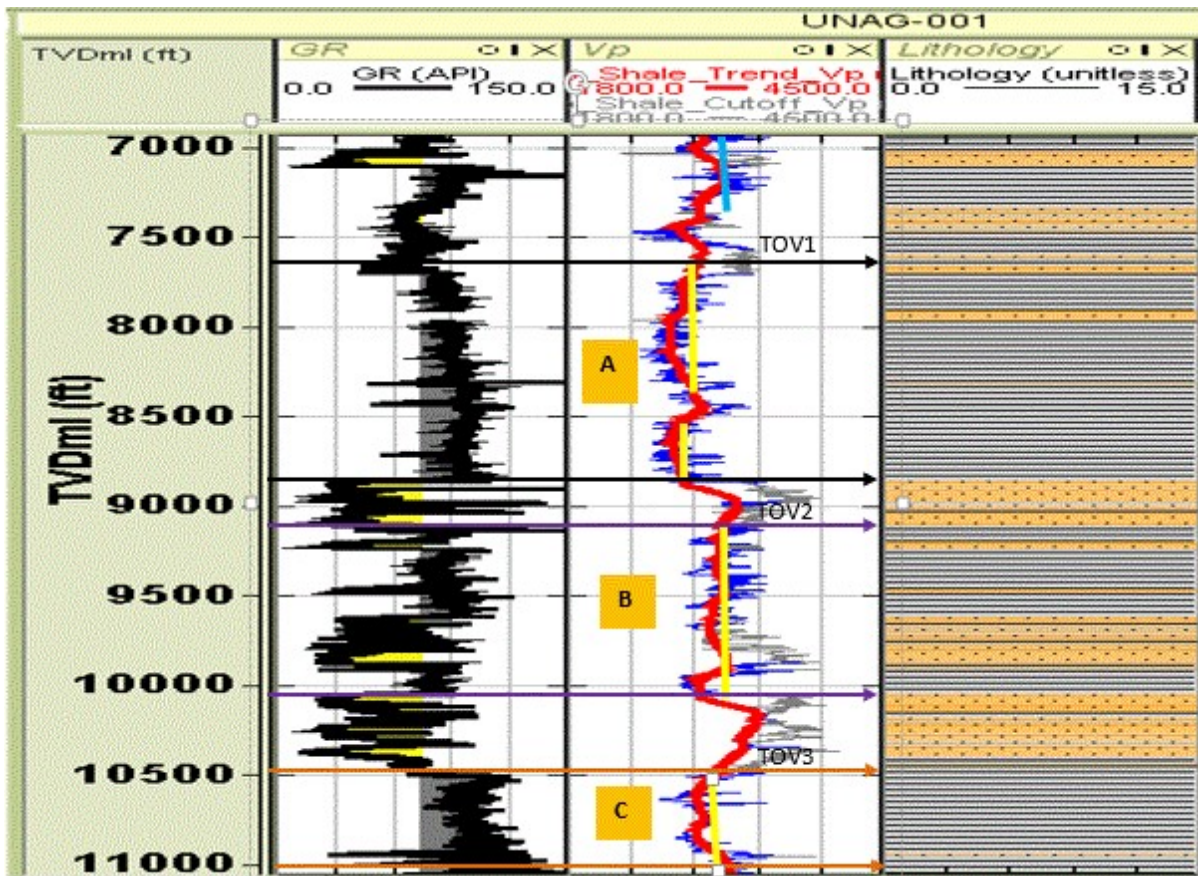
Figure 6: Velocity and Gamma ray logs showing Top of overpressure (TOV1-TOV3) for overpressure zones (A, B and C) and normal compaction (blue line), disequilibrium compaction/under-compaction (yellow line) for Unag-001 well.
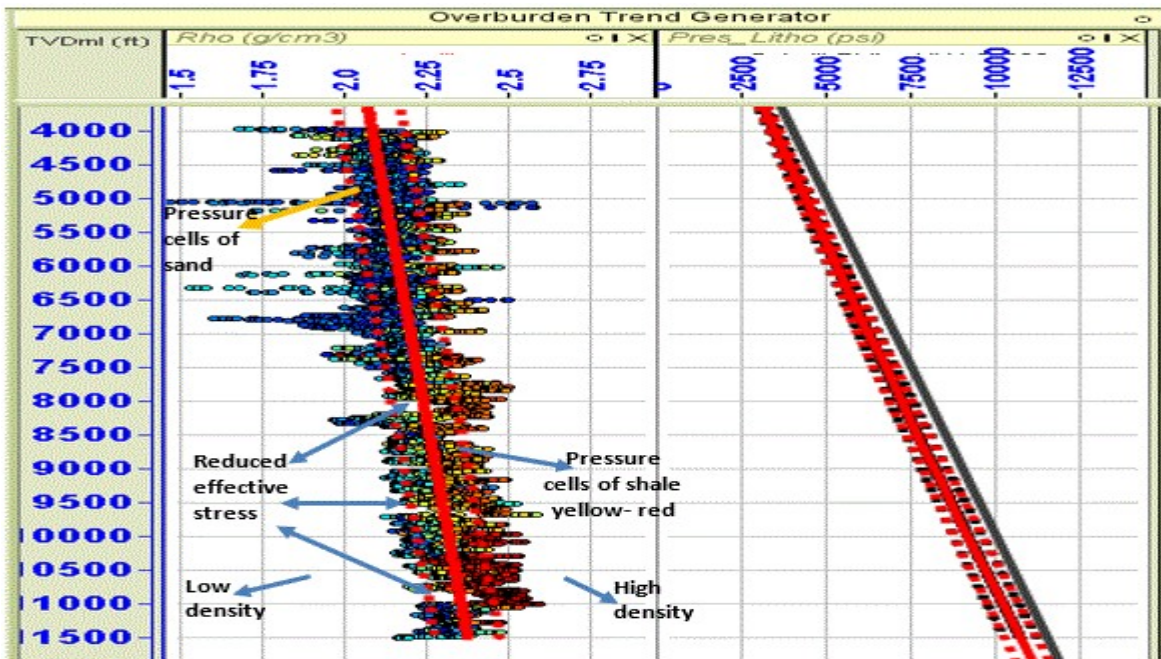
Figure 7: Overburden trend from RHOB (Density) LOG Unag-002 well.
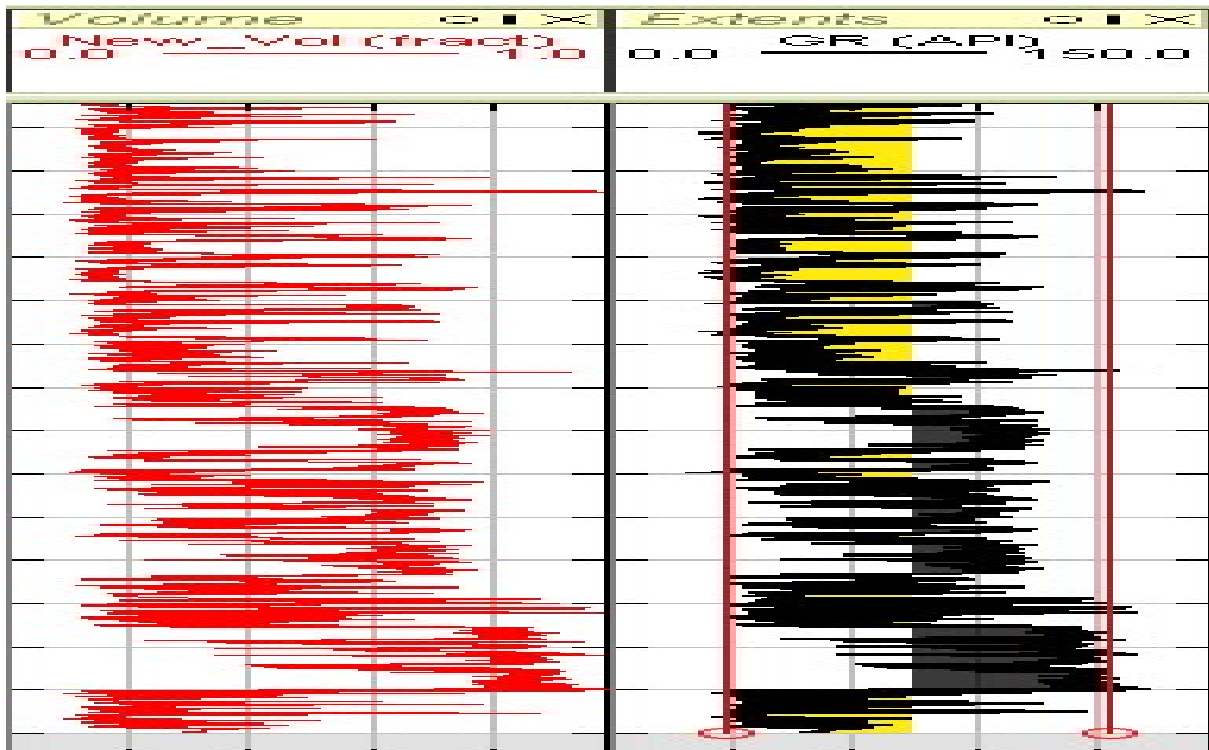
Figure 8: Shale volume log for Unag-002 well.
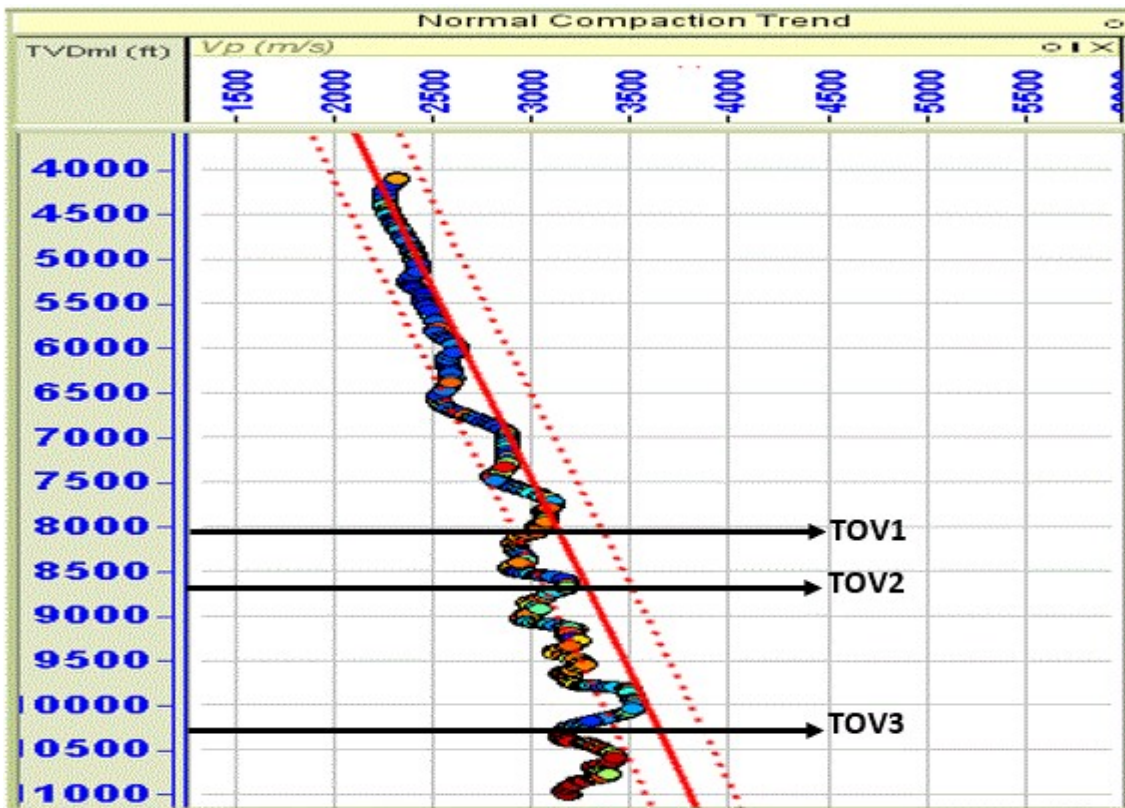
Figure 9: Normal compaction trend (NCT) from Compressional sonic velocity (Vp) log showing top of overpressure in Unag-002 well.
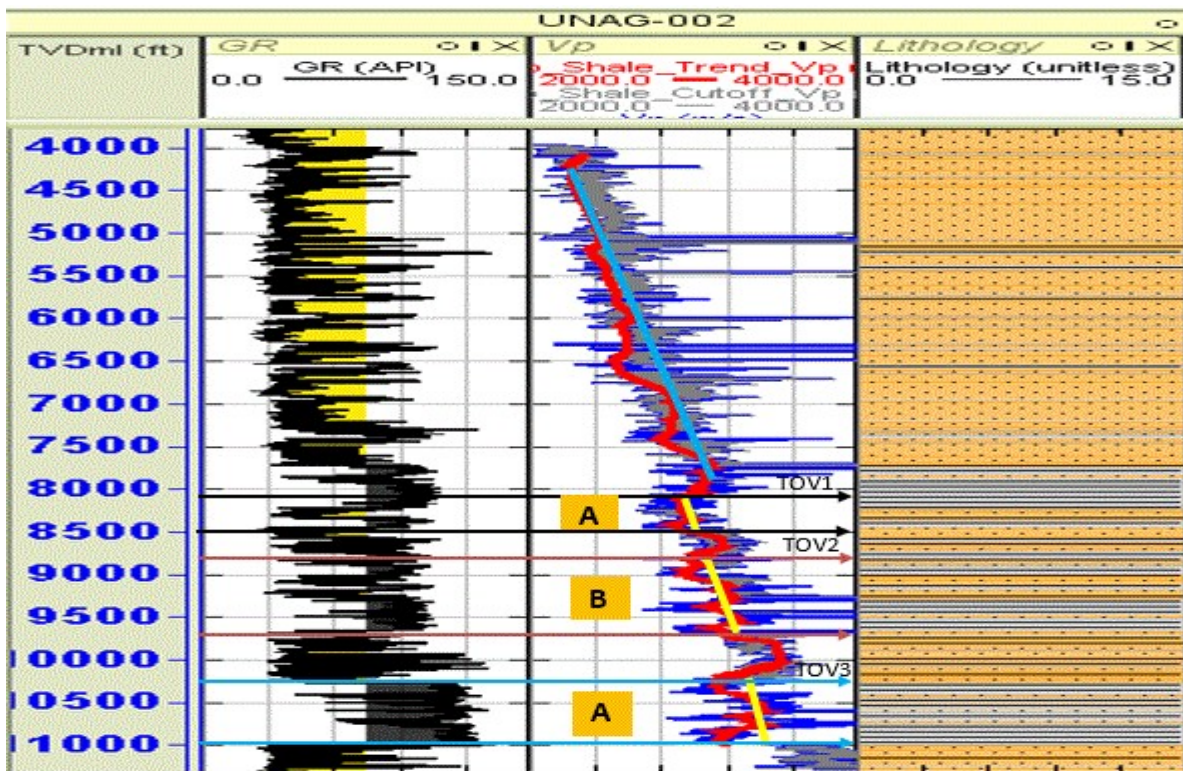
Figure 10: Velocity and Gamma ray logs showing Top of overpressure (TOV1-TOV3) for overpressure zones (A, B and C) and normal compaction (blue line), disequilibrium compaction/under-compaction (yellow line) for Unag-002 well.
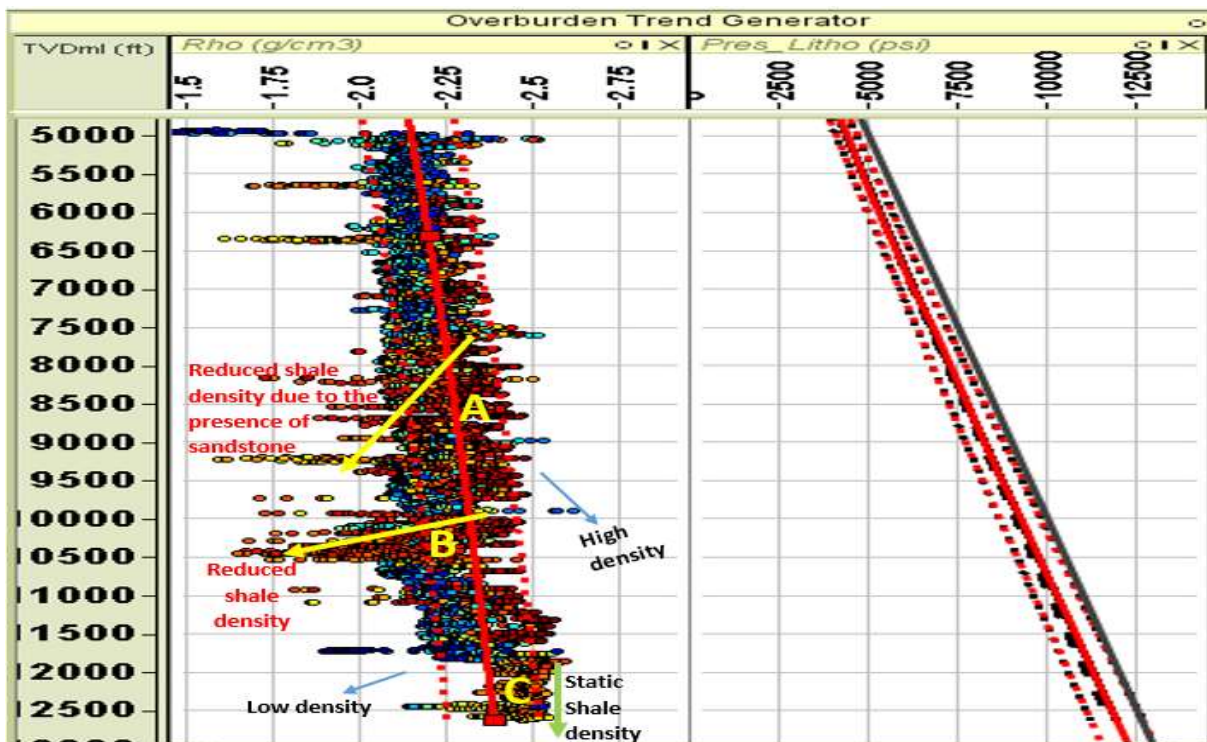
Figure 11: Overburden trend from RHOB (Density) LOG Unag-003 well.
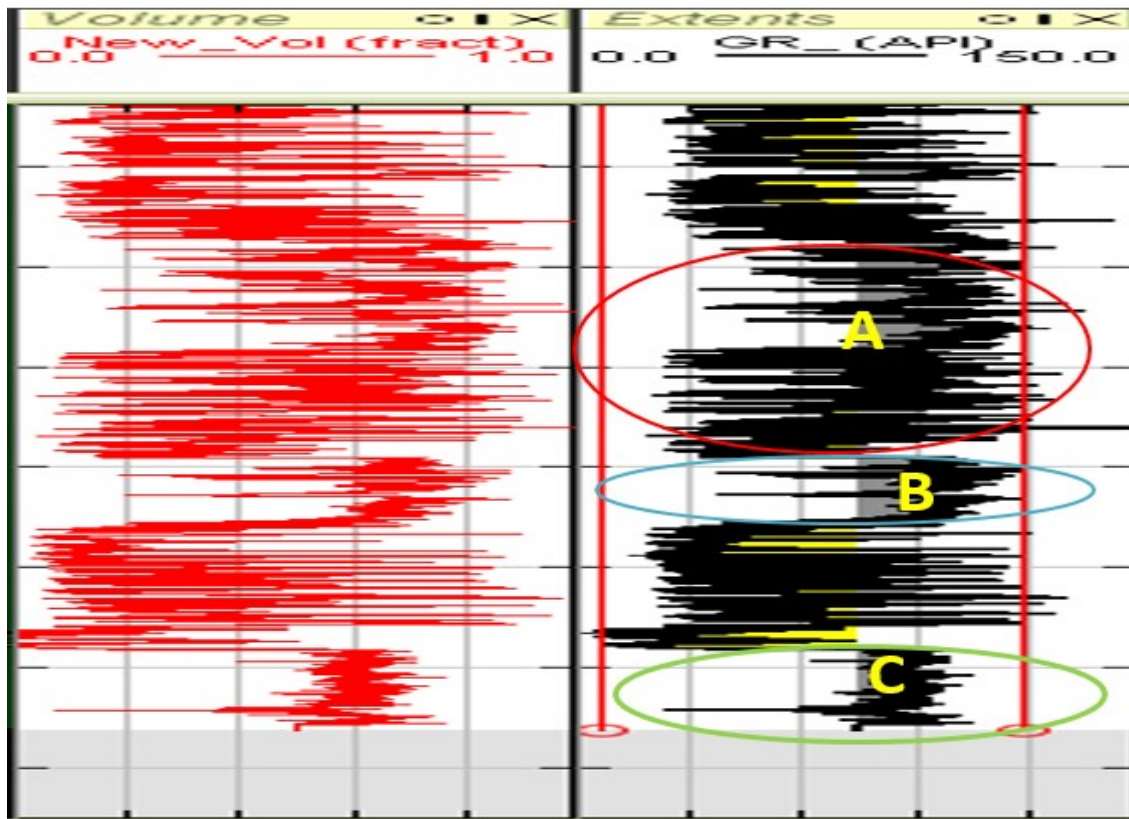
Figure 12: Shale Volume log for Unag-003 Well.
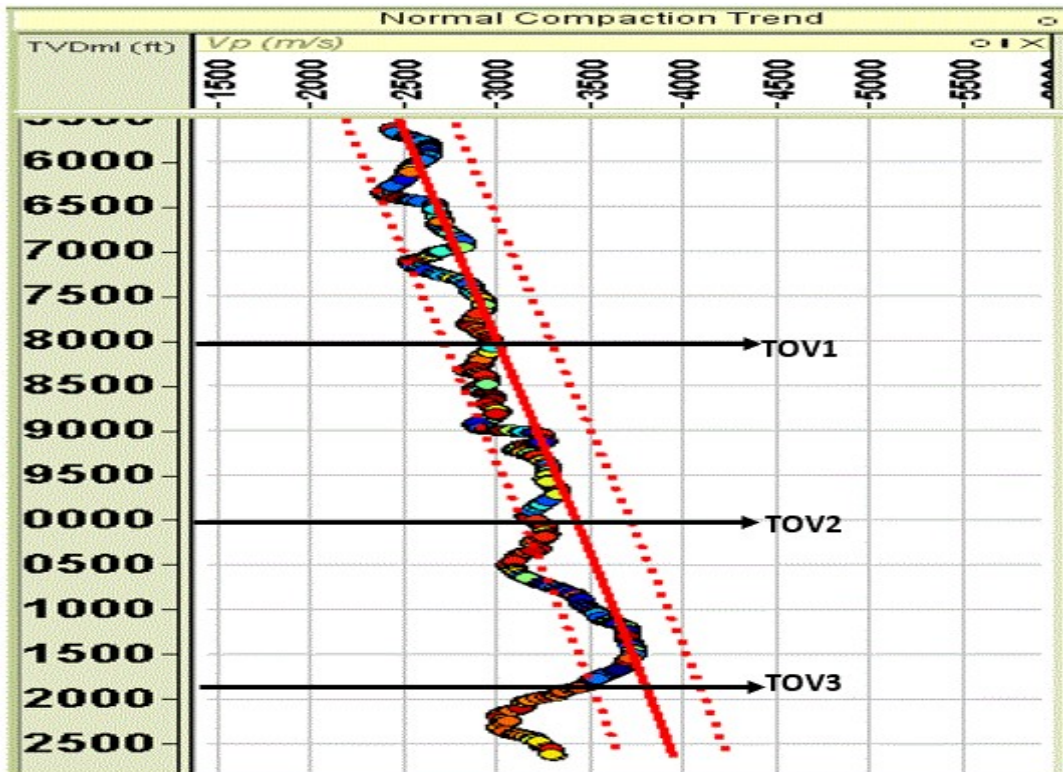
Figure 13: Normal compaction trend (NCT) from Compressional sonic velocity (Vp) log showing top of overpressure in Unag-003 well.
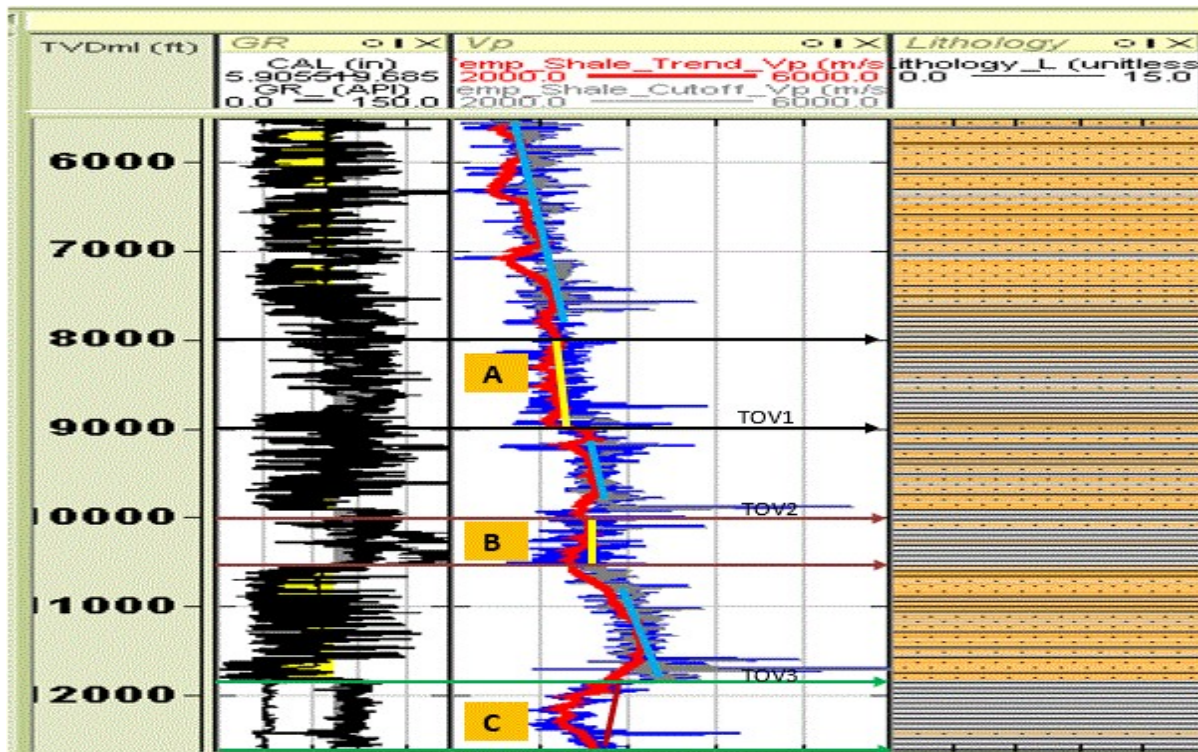
Figure 14: Velocity and Gamma ray logs showing Top of overpressure (TOV1-TOV3) for overpressure zones (A, B and C) and normal compaction (blue line), disequilibrium compaction/under-compaction (yellow line) for Unag-003 well.

V. DISCUSSION OF RESULT

Effective stress and velocity trend methods were employed to produce a detailed prediction of overpressure zones. Density is a function of depth and rate of compaction increases with depth for each lithology. However, shales are more susceptible to compaction because they contain minerals that are less resistive to compaction unlike sandstones which possesses quartz and other resistive minerals. Thus, loss of porosity and increase in density are more prevalent in shale than sandstone bodies within the same depth interval. Thick succession of shale layers at profound depth are denser than their sandstone equivalent due to increased grain contact ratio arising from lack of pore space which may have been squeezed out by compaction from overburden pressure during diagenesis. However, the heterogeneity of subsurface lithology coupled with their varying compaction rate based on the mineralogical constituents of these lithologies, makes well logs deviate from their normal compaction trend at various depth intervals which may wrongly be interpreted as overpressure. Sonic velocity travelling from a clean shale formation to a depth interval of sandy shale, will experience a reduction in velocity due to large porosities present in the sandy shale layer when compared to the overlying shale zone. Therefore, to isolate this ambiguity in identifying overpressure zones, overpressure prediction was centred on shale formation since they are more responsive to overpressure phenomena [2].

Three overpressure zones A, B, and C has been identified across the three wells. In well Unag-001, top of overpressure zones were identified at depths of 7600ft, 9200ft and 10500ft respectively (Figure 5). At depth of 6500 to 8000ft, lithology and shale volume logs shown in Figures 4 and 6 respectively, show alternation of sand/shale zone which appeared like a reduced effective stress on the 2D overburden trend for well-001 (Figure 3), which would have been wrongly interpreted as an overpressure indication. In addition, there were no sharp velocity reversal from its normal compaction trend at the supposed depth of interest in Figure 5. Furthermore, 2D overburden trend for well-001 (Figure 3) showed deflection of pressure cells in the shale zone over to the lower density half of the density best fit line at depths of 11000ft to 12000ft. However, shale volume log for well-001 (Figure 4) showed that there was a sand-shale mixture at this depth which makes bulk density of shale reduce significantly. Therefore, it was inferred that the mechanism of overpressure in well-001, for all the overpressure zones identified is associated to under compaction, since neither density nor effective stress actually reduced.

Overpressure play on the 2D overburden trend in well-002 (Figure 7) were minima and velocity mildly deflected from its normal compaction trend across the three overpressure zones identified in the well. The top of overpressure zones A, B and C for well-002 were identified at 8100ft, 8700ft and 10300ft respectively (Figures 9 and 10). In well-003, top of overpressure zones A, B and C were identified at 8000ft, 10000ft and 11800ft respectively (Figures 13 and 14). But due

to presence of sand, shale density appeared to have dropped in well-003 (Figure 11) at depth range 8000 – 9500ft and 10000 – 10500ft which falls within some parts of overpressure zones A and B identified in this well. In overpressure zone C, shale density remained static as depth increased from 12000 – 12500ft, consequently, shale volume and lithology logs in Figures 12 and 14 collectively show a clean shale zone and a significant reversal in sonic velocity was observed from its normal compaction trend(Figure 13). This observation points to extremely high overpressure due to the fact that density remain constant with depth, thus it was inferred that the mechanism for overpressure in zone C is associated with unloading while the overpressure zones in A and B were associated with under compaction.

The identification of the mechanism of overpressure across wells Unag-001, 002 and 003 were based on [3], method of identification using well logs (Figure 2). The dominant mechanism of overpressure across the overpressure zones is under compaction with exception of overpressure zone C in well-003. Therefore, well-003 has the highest magnitude of overpressure due to occurrence of overpressure from unloading events while well-002 has the least magnitude of overpressure due to slight velocity reversals from its normal compaction trend.

VI. CONCLUSIONS

Velocity method for detecting overpressure is a renowned method in overpressure analysis, due to its optimal level of accuracy in prediction and estimation of overpressures. Effective stress method was also employed to enhance the prediction of the mechanism of overpressure and to check the results derived from large velocity reversals from its normal compaction trend which may sometimes be wrongly identified as high overpressure signals. Three overpressure zones and top of overpressure zones has been identified for well-001, 002 and 003 respectively. The overpressure zones represents depth thickness in which overpressure may have occurred, while top of overpressure represents the depth in which the onset of overpressure began in each overpressure zone identified. The study shows that the overpressure zones A, B and C identified across the three wells, have under compaction as the dominant overpressure mechanism with exceptions to zone C in well-003 which was associated with unloading event.

ACKNOWLEDGEMENT

REFERENCES

[1]. E. Stanley, R.U. Ideozu, A.T. Ibitoye, O.W. Osisanya, and E. Tiekuro., (2018). "Unloading Mechanism: an indication of Overpressure in Niger Delta, 'X'-Field using Cross Plots of rock properties" *International Journal of Applied Physics (SSRG-IJAP)*- 5(2), 25-31.

[2]. G.L. Bowers (2002). "Detecting high overpressure", *The Leading Edge*, 21(2), 174-177.

[3]. S. Chopra, and A. Huffman, (2006). "Velocity determination for pore pressure prediction", *The Leading Edge*, 25(12), 1502 – 1515.

[4]. R.E. Swarbrick, M.J. Osborne, (1998). "Mechanisms that generate abnormal pressures": an overview. In: Law, B.E., Ulmishek, G.F., Slavin, V.I. (Eds.), Abnormal Pressures in Hydrocarbon Environments: *AAPG* Memoir, 70, 13–34.

[5]. M.A. Gutierrez, N.R. Braunsdore, B.A. Couzens, (2006). "Calibration and ranking of Porepressure prediction models", *The leading Edge*, 1516–1523.

[6]. C. Shunhua, X. Yuhong, X, L. Chang, Y. Gangrui, Y.I. Ping, C.A.I. Jun, & X.U. Liqiang, (2006). "Muiltistage approach on pore pressure prediction":*a case study in the South China Sea*. SPE 103856.

[7]. N. Dutta, (2002). "Geopressure prediction using Seismic data: current status and the road ahead, Geophysics, 67(6), 2012-2041.

[8]. K. Terzaghi, (1943). "Theoretical Soil Mechanics", J Wiley and Sons, Inc., University of Michigan, USA,

[9]. B.A. Eaton, (1975). "The Equation for Geopressure Prediction from Well Logs". Society of Petroleum Engineers of AIME. Paper SPE 5544.

[10]. G.L. Bowers, (1995) "Pore pressure estimation from velocity data", accounting for overpressure mechanisms besides undercompaction. SPE Drilling and Completions, June, 1995, pp. 89–95.

[11]. D.A. Obi, A.M. George, and L.O. Ofem, (2018) "Overpressure/Depositional analysis of parts of Onshore (X-Field) Niger Delta Basin Nigeria, Based on well logs data", *Journal of Applied Geology and Geophysics (IOSR-JAGG), Vol 4, Issue 5, DOI:* 10.9790/0990-0405030113, *pp. 01-13.*

[12]. O. Alao, W. Ofuyah, and A. Abegunrin, (2014). "Detecting and Predicting Over Pressure Zones in the Niger Delta, Nigeria: A Case Study of Afam Field", *Journal of Environmental and Earth science; 4(6), pp 13-20.*

[13]. K. W. Ebimobowei, S. Ritu, and J.I. Osazua, (2014). "Modelling seismic velocities and pressure cells for predrill pore pressure prediction and application in development wells in Nigerian deepwater turbidites": *Society of Petroleum Engineers,* pp. 1-12

[14]. T. Reijers, T, (2011). "Stratigraphy and sedimentology of the Niger Delta". *Journal of Geologos*, 17 (6) January-2008: pp. 133-162.

[15]. K.C. Short; A.J. Stauble, (1967). "Outlineofgeologyof NigerDelta".*AAPGBulletin*. 51(5): pp. 761 – 779.

[16]. H. Doust; E. Omatsola; (1990). "NigerDelta,inEdwards,JD; Santogrossi,PA eds; Divergent/passive Margin basins"; *AAPG Memoir* 45: pp. 239–248.

[17]. A.I. Opara, (2010). "Prospectivity Evaluation of "Usso" Field, Onshore Niger Delta Basin, Using 3-D Seismic and Well Log Data", Petroleum & Coal 52 (4), pp. 307-315

[18]. J.O. Etu-Effeotor, (1997). "Fundamentals of Petroleum Geology", Department of Geological Sciences, University of Port-Harcourt, Rivers State, Nigeria. P. 23-65.

[19]. C.N. Nwankwo; J. Anyanwu; S.A. Ugwu, (2014). "Integration of seismic and well log data for petrophysical modeling of sandstone hydrocarbon reservoir in Niger Delta", Sci Afr 13(1), 186–199.

[20]. H. Kulke, (1995). "Regional petroleum Geology of the World", Part II: America, Australia and Antarctica, Berlin Gebruder Bomtraeger, pp. 143–172.

[21]. K.J. Weber, E.M. Daukoru, (1975). "PetroleumGeologyoftheNigerDelta".*Proceedingsofthe 9th World Petroleum Congress Tokyo. Appl. Sci. publishers, Ltd, London.* 2: pp. 202-221.

[22]. A.A. Akpoyovbike, (1978). "Tertiary lithostratigraphy of Niger Delta", *AAPG Bulletin*, 62 (2): P. 295-300.

[23]. B.D. Evamy, J. Haremboure, P. Kamerling, W.A. Knaap, F.A. Molloy, and P.H. Rowlands, (1978). "Hydrocarbon habitat

of Tertiary Niger Delta": *American Association of Petroleum Geologists Bulletin*, Vol. 62, pp. 277- 298

[24]. A.J. Whiteman, (1982). Nigeria: Its petroleum Geology resources and potential 1 and 2. Graham and Trotman, London. 1982; 399.

[25]. A.O. Owoyemi, and A. Wills, (2006). "Depositional patterns across syndepositional normal faults Nigeria", J. Sediment Res 76: 346-363.

[26]. F. Bilotti, and J.H. Shaw., (2005). "Deepwater Niger Delta Fold and Thrust Belt modeled as a Critical – Taper Wedge": The Influence of Elevated Basal Fluid Pressure on Structural Styles". *AAPG Bulletin*. 89(11): p.1475-1491

[27]. T.R. Klett, T.S. Ahlbrandt, J.W. Schmoker, J.L. Dolton J. L., (1997). "Ranking of the Worlds oil and gas provinces by known petroleum volumes", US Geological Survey open-file report 97–463, C.D ROM pp 56–58

[28]. K.K.Nwozor, M.L. Omudu, B.M. Ozumba, C.J. Egbuachor, A.G. Onwemesi, and O.I. Anike, (2013). "Quantitative evidence of secondary mechanisms of overpressure generation": Insights from parts of onshore Niger Delta, Nigeria, petroleum technology development journal, 3(1), p.65-79.

[29]. L.F. Athy, (1930). "Density, Porosity, and compaction of Sedimentary rocks. AAPG Bull. 14 (1), 1-24.

[30]. S.A. Ugwu and C.N. Nwankwo, (2014). "Integrated approach to geopressure detection in the X-field, Onshore Niger Delta: *Journal of Petroleum Exploration Technology", Vol. 4*, pp. 215 – 231.

[31]. J. Zhang, (2011). "Pore pressure prediction from well logs: Methods, modifications, and new approaches", *Elsevier.* Vol.108, ISS.1-2, pp. 50 – 63.